International Journal of Thermophysics, Vol. 12, No. 1, 1991

Viscosity and Thermal Conductivity of Alkali Metal Vapors at Temperatures up to 2000 K

N. B. Vargaftik,[1] Yu. K. Vinogradov,[1] V. I. Dolgov,[1] V. G. Dzis,[1] I. F. Stepanenko,[1] Yu. K. Yakimovich,[1] and V. S. Yargin[1]

Received December 7, 1989

New experimental data were obtained on transport coefficients of alkali metals in gaseous phase at high temperatures and within the pressure range from about 10 to about 100 kPa: lithium—thermal conductivity, $T = 1400$–1800 K, and viscosity, $T = 1600$–2000 K; sodium—viscosity, $T = 1100$–1500 K; and cesium—viscosity, $T = 900$–1250 K. Viscosity of the alkali metal vapors has been measured using a stationary-technique viscometer with an annular gap. Thermal conductivity was measured by the method of the nonstationary monotonous heating. Experimental data were used as a basis for computing effective atom–atom and atom–molecule collision cross section, the values obtained from data on viscosity being in good agreement with those derived from thermal conductivity data. In the case of lithium, the atom–atom cross sections yielded by experiments are fairly consistent with the results of calculations with exact formulae of kinetic theory on the basis of quantum-mechanical potential curves for atom–atom interactions. This has enabled the authors to compile consistent tables of viscosities and thermal conductivities for lithium in a gaseous phase within the temperature range from 800 to 2500 K and pressures from 0.5 to 800 kPa, including the saturation curve.

KEY WORDS: cesium vapor; lithium vapor; sodium vapor; thermal conductivity; viscosity.

1. INTRODUCTION

Experimental studies of the transport coefficients of alkali metals have been limited to temperatures below 1200 K, due primarily to the high chemical activity of those substances. The activity causes the short lifetime of the experimental setup. Use of advanced experimental techniques and high-

[1] Moscow Aviation Institute, Moscow, USSR.

0195-928X/91/0100-0085$06.50/0

temperature structural materials has enabled us to extend the temperature range substantially and to obtain more experimental information.

Combined examination and averaging of the experimental data on viscosity and thermal conductivity has been carried out. The results of theoretical calculation for monatomic vapors starting with the quantum-mechanical potentials of the atom–atom interactions were used in the averaging procedure. This enables us to develop consistent tables of these coefficients, thus improving the dependability of recommended data.

2. THERMAL CONDUCTIVITY OF LITHIUM VAPOR

The thermal conductivity of lithium in the gaseous phase has been measured with the aid of a nonstationary monotonous heating method where, during a single exposure of the sample to monotonous smooth heating (or cooling) within the needed temperature interval, the experiment generates a continuous thermal conductivity curve over the whole interval [1].

The thermal conductivity cell is fabricated from niobium and consists of a rod, 60.124 mm in length and with a radius of 4.774 mm, located coaxially within a cylindrical cavity of the cell. The gap (0.575 mm) between the cavity wall and the rod is filled with the gas under investigation. In operation, with monotonous heating of the cell the heat is transferred mainly through the gas. Based on the available data on heat capacity of the rod, the value of the heat flux can be calculated from the rate of heating of the rod $b_0(T_0) = dT_0/dt$, which is determined by differentiation of an experimental line T_0 vs t, where T_0 is the temperature of the rod, and t is time. To measure temperature drop within the gap four W–Re thermocouples are used. One thermocouple is at the rod axis, and the other three are mounted into the cell body at three different points to take into account the axial nonuniformity of temperature field.

The thermal conductivity, λ, as related to an average temperature of the gas within the gap, was calculated with the formula

$$\lambda = \frac{R_0 \ln R/R_0}{S(1+A)} \frac{Q - Q_\varepsilon - Q_f}{\theta_0 - \theta_c - \theta_j} (1 + \Delta\sigma) \tag{1}$$

where R and R_0 are the radii of the internal surface of the cavity and the rod, respectively, S is the rod surface area, Q is the heat flux to the rod, Q_ε and Q_f represent the corrections for radiation and for parasitic heat flow via the rod fastening members, θ_0 is the temperature drop across the gap, θ_c and θ_j are corrections introduced into the measured drop for the contact resistance of thermocouples at points of fixture and for the temperature

jump, A is the correction for the axial nonuniformity of the temperature field within the cell, and $\Delta\sigma$ is the correction for nonlinearity of heating and the temperature dependence of the thermophysical properties of the cell and of the substance under investigation.

The basic practical difficulties encountered are related mainly to the accuracy of the heat flux Q and the temperature drop θ_0 measured as well as possible to account for all corrections with sufficient accuracy. To calculate the rate of heating $b_0(T_0)$ (and consequently, the heat flux), we used a spline approximation technique. In the case where the function $T(t)$ is defined at discrete points t_i ($i=0, I,..., n$), the problem of smoothing $T(t_i)$ by means of cubic splines is to minimize the functional

$$\Phi(u) = \int_a^b (u'')^2\, dt + \sum_{i=0}^{n} P_i[u(t_i) - T_i]^2 \tag{2}$$

where $u(t)$ is a fitting function built up with simple cubic polynomials in piecemeal fashion, P_i are weights, $a = t_0 < t_1 < \cdots < t_n = b$, and $T_i = T(t_i)$; $u'' = d^2u/dt^2$. The functional combines two conditions: the least "bending" of a curve and the best fitting to experimental points in the sense of the least squares of deviations. The use of a thermal-conductivity cell with sufficiently large thermal inertia eliminates abrupt temperature changes, thus allowing us to draw a smooth heating curve within the accuracy of the T and t values measured, and to obtain reliable values of the derivative dT_0/dt. Specific tests were carried out in vacuum in order to determine the correction for radiative heat transfer. Based on the vacuum results, the value of correction Q_f as well as the gap surface blackness has been calculated at various temperatures. The correction θ_c vs T was determined from calibration measurements with gases with known thermal conductivity. The correction θ_j for the temperature jump at the solid–gas interface was calculated as described in Ref. 2. The values of θ_j did not exceeded 3%.

The problem of suppressing free convection in a vertical annular gap is well developed [3]. Convection is assumed to be absent at $\mathrm{Ra} \leqslant 1000$, where $\mathrm{Ra} = (g\beta\delta^3\rho^2\,\Delta T)/\eta\lambda$ is the Rayleigh number; β. ρ, η, and λ represent compressibility, density, viscosity, and thermal conductivity of the gas, respectively; g is acceleration due to gravity; δ is the gap width, and ΔT is the temperature drop across the gap. Thus, in measuring thermal conductivity, convection was not considered.

The experiments were carried out at isobars of 10, 30, 50, and 80 kPa, at temperatures from 1395 to 1815 K. A number of heating runs were made at each isobar. From the processing of the heating curve with Eq. (1), 223 values for thermal conductivity were determined (see Table I). Average error for the value thus obtained is estimated to be 5%.

Table I. Experimental Data on Lithium Vapor Thermal Conductivity [temperature, T K; thermal conductivity $-\lambda \cdot 10^4$, $W \cdot m^{-1} \cdot K^{-1}$]

T	λ
$P = 10$ kPa	
Series 1	
1395	885
1414	885
1437	890
1460	877
1494	863
1521	880
1550	857
1578	884
1607	864
1636	878
1665	865
1695	878
Series 2	
1402	891
1420	871
1446	865
1473	872
1501	880
1528	865
1556	875
1592	
1621	903
1650	940
1680	916
1710	945
Series 3	
1409	868
1427	874
1453	889
1480	856
1507	870
1535	875
1563	857
1592	852
1621	856
1650	869
1680	873

Table I. *(Continued)*

T	λ
$P = 10$ kPa	
1710	885
1740	897
1763	908
1787	890
1811	921
Series 4	
1414	853
1433	863
1459	860
1487	860
1514	846
1542	841
1570	862
1613	870
1642	872
1672	880
1702	879
1733	883
1756	893
1779	912
1803	915
Series 5	
1495	897
1523	869
1552	889
1573	880
1595	885
1616	891
1638	888
1660	923
1682	948
1704	963
1727	964
1749	967
1773	953
1796	945
Series 6	
1428	902
1455	873
1479	837

Table I. *(Continued)*

T	λ
$P = 10$ kPa	
1507	828
1535	821
1557	842
1579	865
1604	880
1629	881
1651	892
1669	885
1688	893
1706	911
1725	910
1740	915
1756	920
1767	923
1778	923
1790	938
Series 7	
1483	830
1496	835
1509	841
1523	844
1544	853
1564	841
1586	843
1607	873
1629	880
1651	884
1673	902
1695	906
$P = 30$ kPa	
Series 1	
1510	954
1524	934
1538	922
1552	923
1566	911
1580	911
1594	914
1608	927
1623	948

Table I. *(Continued)*

T	λ
$P = 30$ kPa	
1637	933
1652	921
1673	932
1696	944
1718	941
1740	951
1763	954
1786	967
1801	961
Series 2	
1528	959
1550	952
1571	951
1593	939
1614	921
1636	912
1658	912
1680	911
1695	914
1714	916
1732	940
1748	951
1763	937
1779	960
1790	949
1802	958
1814	971
Series 3	
1505	922
1524	933
1545	940
1572	920
1601	929
1629	927
1659	911
1688	903
1718	927
1742	935
1766	936
1781	923

Table I. *(Continued)*

T	λ
$P = 30$ kPa	
Series 4	
1498	993
1517	974
1537	966
1565	955
1593	955
1622	935
1651	949
1681	937
1711	945
1734	924
1757	929
1781	937
1797	942
$P = 50$ kPa	
Series 1	
1594	968
1616	965
1638	959
1660	950
1682	941
1704	950
1727	951
1749	955
1772	946
1795	940
Series 2	
1581	970
1595	968
1609	9700
1623	972
1638	972
1652	966
1667	954
1681	948
1696	938
1711	936
1733	941
1756	949

Table I. *(Continued)*

T	λ
$P = 50$ kPa	
1779	954
1798	973
1814	981
Series 3	
1554	1015
1573	985
1594	989
1615	978
1644	966
1674	986
1696	981
1718	998
1741	985
1765	978
1781	973
Series 4	
1561	995
1580	1008
1601	992
1629	973
1659	963
1688	979
1711	967
1734	956
1759	982
1773	989
$P = 80$ kPa	
Series 1	
1639	1006
1660	998
1682	997
1704	984
1727	983
1750	988
1773	969
1796	966
Series 2	
1618	1033
1638	1018

Table I. *(Continued)*

T	λ
$P = 80$ kPa	
1660	1028
1682	1028
1704	1011
1726	1018
1749	1008
1772	1007
1796	1009

3. VISCOSITY OF LITHIUM, SODIUM, AND CESIUM VAPORS

The viscosity of lithium, sodium, and cesium vapors has been measured by a capillary-flow method with a short narrow annular channel as a measuring cell [4, 5]. The working formula was developed on the base of the generalized Bernoulli equation for isothermal flow of a real compressible fluid assuming that for viscous loss within the section of fully developed flow, Poiseuille's law holds (the condition of laminar flow is met for Reynolds number values of 20 to 50 typical for runs with vapors under investigation). The viscosity was computed from the flow rate through a measured section of the capillary. The flow rate, in turn, is determined from the condensate accumulation rate within a calibrated cylindrical vessel (flow meter). The main advantage of the method is that it enables one to solve easily the significant problem of creating a uniform temperature field over the entire length of the measuring element.

A measuring cell made of Nb–Zr–C alloy [5, 6] was used in this experiment. Geometrical parameters of the annular channel are as follows: internal diameter, 5.00 mm; annual gap width, 0.16 mm; and length of the measuring section, 26.0 mm.

The experimental and measurement techniques as well as the calibration procedure have been described in detail in previous papers [5, 6]. Also, in Ref. 5 we considered the problems related to local losses at the channel entrance and the existence of a channel section with undeveloped flow.

Since the error in the viscosity is due primarily to the uncertainty in the flow rate, the major attention was payed to measuring the vapor flow-rate values. This quantity was determined from the inclination of the condensate elevation level, h, within the flow meter versus time, t. The error of

the flow rate computation was determined from the spread of points relative to the averaging straight line $h(t)$. The stability of the flow rate was monitored, yielding acceptable standard deviations and, hence, acceptable accuracy of the resulting flow rate.

The viscosity of lithium, sodium, and cesium in the gaseous phase has been measured in the pressure range from about 10 to 100 kPa and at temperatures of 1600–2000, 1100–1500, and 900–1250 K, respectively. The experimental results are presented in Table II. To compute the vapor composition [7] we have used the following values of the dissociation energies of the diatomic molecules [8]:

$$D^0_{0_{Li}} = 107{,}800 \pm 1300 \text{ J} \cdot \text{mol}^{-1}$$

$$D^0_{0_{Na}} = 71{,}380 \pm 850 \text{ J} \cdot \text{mol}^{-1}$$

$$D^0_{0_{Cs}} = 44{,}380 \pm 1000 \text{ J} \cdot \text{mol}^{-1}$$

The errors in the measured viscosity were calculated taking into account the errors in the measured vapor flow rate at the completion of a run for given temperature and pressure. The resulting viscosity errors differ for different experimental points and vary from 2.2 to 4.2%, the mean error being 3% for all metals investigated.

4. REPRESENTATION OF EXPERIMENTAL DATA

The experimental data for the thermal conductivity and viscosity were approximated with the following relationships, which were developed on the basis of the transport process theory for a rarefied dissociating binary gaseouos mixture [9]:

$$\lambda(x_2, T) = \lambda_1(T) \frac{1 + a_1 x_2 + a_2 x_2^2}{1 + a_3 x_2 + a_4 x_2^2} + \frac{a_5 x_2}{1 + a_6 x_2} + a_7 \left(\frac{D_0(T)}{RT} \right)^2 \frac{x_2(1 - X_2)}{(1 + x_2)^2} \tag{3}$$

$$\eta(x_2, T) = \eta_1(T) \frac{1 + b_3 x_2 + b_4 x_2^2}{1 + b_1 x_2 + b_2 x_2^2} \tag{4}$$

Here λ_1 and η_1 represent the thermal conductivity and viscosity of monatomic vapor, $D_0(T)$ is the dissociation energy at temperature T, x_2 is the mole fraction of diatomic molecules, coefficients a_i and b_i are uniquely determined [9] by the same quantity, namely, by the relative atom–

Table II. Experimental Data on Viscosity of Lithium, Sodium, and Cesium in the Gaseous Phase[a]

No. 1	T (K), 2	P (kPa), 3	$\eta \cdot 10^7$ (Pa·s), 4	ΔP (kPa), 5	x_2 (%), 6	$\rho \cdot 10^2$ (kg·m^{-3}) 7	τ (min·s^{-1}), 8	h (mm), 9	σ_θ/θ (%), 10
					Lithium				
1	1595	21.7	163	1.47	3.51	1.17	153/36	12.0	1.63
2	1607	73.8	143	1.96	9.78	4.21	101/18	40.3	0.42
3	1613	19.7	176	1.40	2.93	1.05	160/18	9.92	0.78
4	1615	72.8	144	2.13	9.34	4.12	115/25	48.6	0.53
5	1636	58.6	158	1.99	7.08	3.20	120/36	34.0	0.53
6	1656	14.8	181	1.42	1.81	0.76	111/47	5.11	1.80
7	1668	23.9	187	1.88	2.70	1.23	150/18	12.3	1.75
8	1692	41.2	174	1.65	4.02	2.12	133/27	19.00	0.78
9	1700	22.6	183	1.50	2.21	1.14	168/13	11.5	1.42
10	1715	71.3	166	2.02	5.99	3.68	128/36	39.9	0.78
11	1722	98.3	160	2.18	7.71	5.14	40/10	19.4	0.27
12	1747	26.0	195	1.18	2.05	1.27	150/51	8.43	0.78
13	1812	84.9	184	2.13	4.77	4.10	133/18	43.9	0.63
14	1815	21.5	193	1.14	1.28	1.00	169/13	7.40	1.28
15	1823	47.4	193	2.01	2.66	2.23	150/33	24.9	1.44
16	1830	65.0	192	2.01	3.48	3.07	150/40	34.0	0.63
17	1852	89.9	186	1.75	4.33	4.23	161/50	44.9	1.02
18	1970	54.9	210	1.59	1.78	2.13	150/15	19.2	0.27
19	1983	106.8	208	2.51	3.22	4.64	98/25	38.4	0.78
					Sodium				
1	1115	18.3	209	1.55	3.45	4.70	71/18	10.0	1.02
2	1119	12.0	217	1.91	2.26	3.04	70/13	8.02	1.02
3	1123	12.0	212	1.49	2.20	3.03	159/18	14.1	0.74
4	1109	25.8	200	2.17	4.92	6.74	46/27	13.3	0.53
5	1216	56.2	226	2.83	5.18	13.4	40/37	26.3	1.28
6	1212	57.1	219	1.73	5.37	13.7	50/05	20.7	0.78
7	1201	32.9	229	1.80	3.45	7.83	50/09	12.0	0.78
8	1211	14.2	240	1.75	1.45	3.28	129/22	12.9	1.34
9	1209	17.1	227	1.95	1.77	3.99	105/26	14.8	1.09
10	1206	71.8	213	1.99	6.81	17.6	63/18	39.5	0.27
11	1336	99.5	240	1.78	4.71	21.6	38/19	23.2	1.09
12	1342	99.5	250	1.78	4.58	21.4	35/00	20.2	1.02
13	1325	49.4	250	1.83	2.58	10.6	48/09	14.2	0.53

[a] T, average temperature in the experiment; P, average pressure along the length of the measuring element of the viscometer; ΔP, pressure drop across the measuring element; x_2, mole fraction of diatomics; ρ, vapor density at specified T and P; τ, total condensate accumulation time; h, total condensate level elevation within the effective portion of the flowmeter (diameter 28 mm); σ_θ/Q, relative mean-square deviation of the measured vapor flow rate.

Table II. *(Continued)*

No. 1	T (K), 2	P (kPa), 3	$\eta \cdot 10^7$ (Pa·s), 4	ΔP (kPa), 5	x_2 (%), 6	$\rho \cdot 10^2$ (kg·m^{-3}) 7	τ (min·s^{-1}), 8	h (mm), 9	σ_θ/θ (%), 10
14	1356	18.1	260	1.55	0.84	3.72	100/35	9.21	1.22
15	1399	50.1	266	1.98	1.85	10.1	59/18	17.3	0.53
16	1406	96.2	264	1.92	3.33	19.6	57/11	31.0	1.28
17	1404	68.7	252	1.29	2.44	13.8	49/14	13.4	0.74
18	1413	28.3	261	2.21	0.99	5.59	62/08	11.8	0.95
19	1389	28.3	268	2.21	1.11	5.69	65/10	12.3	0.42
20	1511	99.8	284	1.45	2.24	18.7	42/10	15.2	0.63
21	1510	60.8	287	2.64	1.39	11.3	35/10	14.2	1.87
22	1513	90.1	282	2.01	2.01	16.8	69/15	31.6	0.63
23	1524	78.2	285	1.75	1.68	14.4	57/12	19.4	0.78
24	1520	70.6	284	1.41	1.55	13.1	52/14	12.9	0.78
25	1145	36.2	209	1.81	5.30	9.20	50/04	15.4	1.34
26	1162	25.8	215	2.19	3.39	6.35	135/35	34.8	0.95
27	1248	83.8	223	1.75	6.23	19.7	48/11	28.0	1.64
28	1281	25.8	249	2.10	1.74	5.66	45/09	8.60	1.22
					Cesium				
1	903	12.0	266	0.90	1.49	21.6	110/09	17.2	0.86
2	906	13.4	265	1.00	1.62	24.0	68/26	13.3	0.54
3	911	15.8	264	0.83	1.85	28.3	56/16	10.5	0.48
4	916	40.4	254	1.92	4.31	73.5	28/50	13.6	0.37
5	916	48.5	253	1.75	5.11	89.1	19/20	14.3	0.49
6	920	51.7	252	1.27	5.27	94.4	17/55	16.8	0.83
7	921	56.2	247	1.47	5.64	104.0	23/34	28.2	1.08
8	917	26.6	264	1.61	2.90	47.6	29/13	17.9	0.50
9	924	52.2	251	1.70	5.17	95.5	7/50	9.78	0.63
10	1038	46.5	289	1.18	2.47	73.4	20/74	12.5	1.08
11	1031	52.2	289	0.90	2.85	83.2	46/05	24.0	1.08
12	1045	47.7	286	1.65	2.43	74.7	17/28	15.1	0.64
13	1048	39.0	296	0.78	1.98	60.1	32/28	10.7	0.39
14	1052	108.7	279	0.53	5.06	173.0	42/24	27.8	0.70
15	1052	122.6	276	1.08	5.64	197.0	14/16	24.4	0.42
16	1054	88.0	288	0.74	4.13	138.0	38/24	27.3	0.38
17	1040	67.1	287	1.00	3.44	107.0	37/12	27.5	0.32
18	1055	76.5	283	1.14	3.64	121.0	27/53	26.4	1.80
19	1054	73.8	289	1.16	3.46	115.0	25/48	23.5	0.21
20	1057	76.6	283	1.85	3.58	120.0	10/27	15.9	0.25
21	1059	101.0	281	1.08	4.58	159.0	21/07	25.1	0.45
22	1134	51.4	299	1.50	1.76	74.2	9/12	25.5	0.10
23	1129	87.2	300	0.66	2.91	127.0	41/52	23.9	0.86
24	1128	119.7	305	0.73	3.92	176.0	119/47	16.7	0.31
25	1136	66.2	296	1.38	2.22	95.8	11/18	23.9	0.86
26	1133	132.9	297	1.64	4.23	196.0	19/33	40.0	0.24

Table II. *(Continued)*

No. 1	T (K), 2	P (kPa), 3	$\eta \cdot 10^7$ (Pa·s), 4	ΔP (kPa), 5	x_2 (%), 6	$\rho \cdot 10^2$ (kg·m^{-3}) 7	τ (min·s^{-1}), 8	h (mm), 9	σ_θ/θ (%), 10
27	1134	18.5	319	0.85	0.63	26.3	46/19	7.02	0.21
28	1139	31.4	316	1.68	1.04	44.7	43/39	21.7	0.61
29	1139	70.2	304	1.78	2.22	101.0	18/48	21.9	0.38
30	1142	102.0	299	1.52	3.18	148.0	25/28	37.2	0.70
31	1136	101.5	302	0.77	3.25	147.0	29/23	21.1	0.31
32	1138	29.2	307	0.69	0.97	41.5	52/22	10.1	0.69
33	1143	112.8	301	1.26	3.48	164.0	18/54	25.4	0.67
34	1139	66.8	308	0.79	2.16	95.9	23/25	11.9	0.49
35	1152	52.7	309	1.54	1.62	74.1	45/10	33.9	0.88
36	1232	116.9	326	0.84	2.51	155.0	22/45	18.5	0.28
37	1235	132.3	324	0.90	2.81	176.0	33/22	32.8	0.34
38	1239	91.2	335	1.16	1.94	120.0	15/23	12.9	0.39
39	1240	107.1	320	1.36	2.26	141.0	26/60	32.3	0.68
40	1241	80.0	316	1.17	1.71	105.0	20/14	15.2	1.73
41	1245	109.8	339	2.29	2.27	144.0	9/54	18.7	1.05

molecule collision cross section $\beta_{12}^2 = [\sigma_{12}^2 \Omega_{12}^{(2,2)*} / \sigma_{11}^2 \Omega_{11}^{(2,2)*}]$, where $\sigma_{11}^2 \Omega_{11}^{(2,2)*}$ and $\sigma_{12}^2 \Omega_{12}^{(2,2)*}$ are effective atom–atom and atom–molecule collision cross sections, respectively. Also, from the well-known formula [Ref. 10, Eqs. (8.2-18) and (8.2-31)], η_1 and λ_1 at the temperature T are related only to cross section $\sigma_{11}^2 \Omega_{11}^{(2,2)*}$. Consequently, the extraction of the cross sections $\sigma_{11}^2 \Omega_{11}^{(2,2)*}$ and β_{12}^2 from the experimental data gives us a chance to generalize thermal conductivity and viscosity data.

As is well known [9], the relations $\lambda_1(T)$ and $\eta_1(T)$ exhibit linear behavior over the whole temperature range dealt with. Thus, in processing experimental data, relative cross section β_{12}^2 and linearity coefficients for $\eta_1(T)$ or $\lambda_1(T)$ constitute approximation parameters. The results of approximation performed by the least-squares method are as follows.

For lithium

$$\lambda_1 = [541.0 + 0.485(T - \Delta 1000)] \cdot 10^{-4}, \quad \mathrm{W \cdot m^{-1} \cdot K^{-1}}; \quad \beta_{12}^2 = 4.5 \pm 0.4 \tag{5}$$

$$\eta_1 = [129.1 + 0.100(T - 1000)] \cdot 10^{-7}, \quad \mathrm{Pa \cdot s}; \quad \beta_{12}^2 = 3.2 \pm 0.4 \tag{6}$$

For sodium

$$\eta_1 = [208.1 + 0.155(T - 1000)] \cdot 10^{-7}, \quad \mathrm{Pa \cdot s}; \quad \beta_{12}^2 = 2.3 \pm 0.4 \tag{7}$$

For cesium

$$\eta_1 = [289.5 + 0.240(T - 1000)] \cdot 10^{-7}, \quad \text{Pa} \cdot \text{s}; \quad \beta_{12}^2 = 2.1 \pm 0.4 \tag{8}$$

Effective atom–atom collision cross sections $\sigma_{11}^2 \Omega_{11}^{(2,2)*}$ are calculated from the relations for $\lambda_1(T)$ and $\eta_1(T)$ [Ref. 10, Eqs. (8.2-18) and (8.2-31)].

5. DISCUSSION OF EXPERIMENTAL RESULTS. TABULATION

The curves $\sigma_{11}^2 \Omega_{11}^{(2,2)*}$ vs T for lithium and sodium vapors are plotted in Figs. 1 and 2, respectively. The solid lines represent the results derived from the experimental data on λ and η, while the dashed lines represent the calculation from kinetic theory on the basis of quantum-mechanical potential curves for atom–atom interactions. All calculations [11–14] used, in

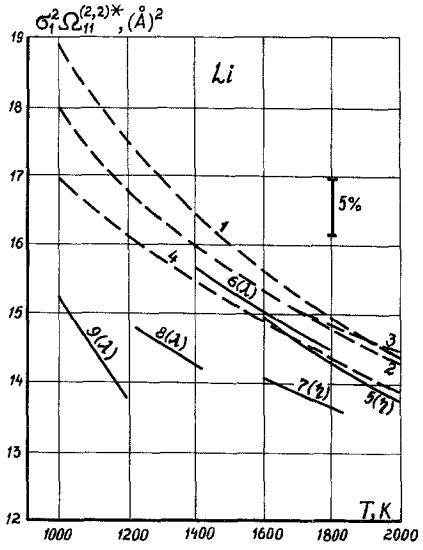

Fig. 1. Effective atomic collision cross section $\sigma_{11}^2 \Omega_{11}^{(2,2)*}$ in lithium vapor. Solid lines, as derived from experimental data; dashed lines, calculations on the basis of quantum-mechanical potential curves. 1–3, numerical integration with exact formulae of kinetic theory [11–13]; 4, computation by approximation method [9]; 5, results of the present study (viscosity); 6, results of the present study (thermal conductivity); 7–9, results given in Refs. 4 and 19.

practice, the same data on atom–atom interaction potentials as in Refs. 15–18.

As can be seen from Fig. 1, the value of $\sigma_{11}^2 \Omega_{11}^{(2,2)*}$ extracted from our experiments on viscosity and thermal conductivity of lithium vapor are in good agreement with each other. As compared to other experiments for the thermal conductivity and viscosity [4], the present cross sections are 5–8% higher, which is within the data error limits of Ref. 4. The cross sections calculated from the experimental results on thermal conductivity of Ref. 19 are significantly lower and their temperature dependence is drastically different from those given in other publications. These discrepancies seem to be explained by the very large corrections introduced into the thermal conductivity data of [19] during experimental results processing. The cross sections $\sigma_{11}^2 \Omega_{11}^{(2,2)*}$ obtained by the authors confirm the computational results of Refs. 11–13 (discrepancies are less than 3%).

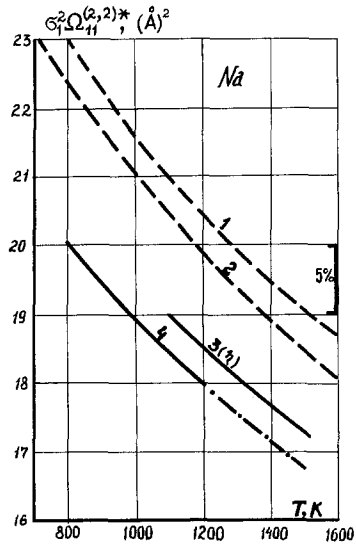

Fig. 2. Effective atomic collision cross section $\sigma_{11}^2 \Omega_{11}^{(2,2)*}$ in sodium vapor. Solid lines, as derived from experimental data; dashed lines, calculations on the base of quantum-mechanical potential curves. 1 and 2, numerical integration with exact formulae of kinetic theory [13, 14]; 3, results of the present study (viscosity); 4, generalization of experimental data [9] on viscosity and thermal conductivity (dash-dot curve, extrapolation).

The values of β_{12}^2 found from the thermal-conductivity and viscosity data are also in good agreement with each other. The difference between them does not exceed the tolerance for β_{12}^2 determined by the tolerance for dissociation energy [8].

Similar results for sodium vapor are given in Fig. 2. Our values of $\beta_{11}^2 \Omega_{11}^{(2,2)*}$ are in agreement within the limits of 3% with the results of the averaging of all the available experimental data on viscosity and thermal conductivity of sodium vapor [9]. On the other hand, these cross sections in experimental temperature range are 7–9% lower than those found through computations of Refs. 13 and 14, thus falling within the limits of the summarized error of experimental and computational data. Discrepancies between the experimental and the calculated atom–atom cross sections for sodium are consistently larger than for lithium. It should be noted, however, that for sodium, available theoretical atom–atom interaction potentials have a much lower accuracy than those for lithium [20]. In the case of cesium, the atom–atom cross sections found by the authors agree within the error lilmits with the averaging curve from Ref. 9.

Having made a combined analysis of data on viscosity and thermal conductivity of lithium vapor obtained, we developed tables of recom-

Table III. Thermal Conductivity of Lithium in the Gaseous Phase, $\lambda \cdot 10^4$, $W \cdot m^{-1} \cdot K^{-4}$ (Recommended Data)

		P (kPa)											
T (K)	λ_1	0.5	1	5	10	30	80	100	200	400	600	800	λ_{sat}
800	450												543
900	506												652
1000	558												753
1100	607	828											841
1200	655	731	795										913
1300	701	728	753	915									966
1400	745	756	767	842	916								1003
1500	790	795	799	834	873	984							1029
1600	834	836	839	855	874	939	1034						1045
1700	878	879	800	888	897	932	955	1012					1055
1800	921	922	922	926	930	948	984	996	1036				1058
1900	965	965	966	967	969	978	997	1003	1029	1054			1058
2000	1008	1008	1009	1009	1010	1014	1022	1025	1038	1054	1059	1056	1054
2100	1050	1050	1050	1050	1050	1051	1053	1054	1059	1064	1066	1064	1048
2200	1092	1092	1092	1092	1092	1091	1090	1090	1088	1086	1083	1080	1041
2300	1131	1131	1131	1131	1130	1129	1126	1125	1120	1102	1106	1099	1031
2400	1169	1169	1169	1168	1168	1166	1162	1161	1155	1143	1133	1122	1020
2500	1203	1203	1203	1202	1202	1201	1196	1195	1187	1173	1162	1152	1006

mended values for these coefficients (see Tables III and IV). In the tables we have utilized the results of computations for $\sigma_{11}^2 \Omega_{11}^{(2,2)*}$ given in Ref. 12 for establishing $\eta_1(T)$ and $\lambda_1(TG)$. As to relative cross sections β_{12}^2, we have taken the values extracted from corresponding experimental data, viz., $\beta_{12}^2 = 3.2$, for viscosity and $\beta_{12}^2 = 3.5$ for thermal conductivity. As mentioned above, these values of β_{12}^2 are in good agreement with each other. As a result the following values have been obtained for coefficients a_i and b_i in Eqs. (3) and (4), corresponding to the specified values of β_{12}^2 and x_2 calculated for $D_0^0 = 107{,}800\ \mathrm{J \cdot mol^{-1}}$ [8]:

$$a_1 = -0.023; \quad a_2 = -0.322; \quad a_3 = 4.020; \quad a_4 = 1.948;$$
$$a_5 = 0.214; \quad a_6 = -1.631; \quad a_7 = .095;$$
$$b_1 = 4.094; \quad b_2 = 3.335; \quad b_3 = 0.864; \quad b_4 = -6.964 \times 10^{-2}$$

Tables of recommended data on viscosity and thermal conductivity of sodium and cesium vapors will be compiled upon the completion of experiments on thermal conductivity.

Table IV. Viscosity of Lithium in Gaseous Phase, $\eta \cdot 10^7$, Pa · s (Recommended Data)

		P (kPa)											
T (K)	η_1	0.5	1	5	10	30	80	100	200	400	600	800	λ_{sat}
800	100												97.2
900	112												106
1000	123												113
1100	134	119											118
1200	145	139	133										123
1300	155	152	149	131									126
1400	166	164	163	152	142								129
1500	176	175	174	168	161	141							131
1600	186	185	185	181	176	170	137						133
1700	196	196	195	193	190	179	159	153					135
1800	205	205	204	203	200	193	177	172	152				137
1900	215	215	214	214	212	206	194	190	173	149			139
2000	224	224	223	223	222	218	208	205	190	169	154	143	140
2100	233	233	233	232	232	229	221	218	206	187	173	162	141
2200	242	242	242	241	240	238	232	230	220	203	190	180	143
2300	250	250	250	249	249	247	242	241	232	218	206	196	144
2400	260	260	160	259	259	258	253	253	245	233	222	213	146
2500	268	268	268	267	267	266	263	261	256	245	236	227	147

REFERENCES

1. Yu. K. Vinogradov and N. I. Sidorov, *Teplofiz. Vysokikh Temp.* **20**:1158 (1982).
2. V. V. Makhrov, *Teplofiz. Vysokikh Temp.* **15**:539 (1977); **15**:1183 (1977); **16**:737 (1978).
3. K. Kraussold, *Forsch. Ing. Wes.* **5**:94 (1934).
4. N. B. Vargaftik, V. S. Yargin, N. I. Sidorov, Y. V. Tarlakov, V. I. Dolgov, V. M. Kapitonov, and A. A. Voschinin, *High Temp. High Press.* **16**:57 (1984).
5. I. F. Stepanenko, N. I. Sidorov, Y. N. Tarlakov, and V. S. Yargin, *Int. J. Thermophys.* **7**:829 (1986).
6. I. F. Stepanenko, N. I. Sidorov, Y. V. Tarlakov, and V. S. Yargin, *Izmeritelnaya Tekhnika* **8**:62 (1987).
7. N. B. Vargaftik and L. D. Volyak, in *Handbook of Thermodynamic and Transport Properties of Alkali Metals*, R. W. Ohse, ed. (Blackwell, Oxford, 1985), pp. 535–576.
8. N. B. Vargaftik, *Tables on the Thermophysical Properties of Liquids and Gases* (Hemisphere, Washington–London, 1978).
9. N. B. Vargaftik, V. S. Yargin, in *Handbook of Thermodynamic and Transport Properties of Alkali Metals*, R. W. Ohse, ed. (Blackwell, Oxford, 1985), pp. 785–842.
10. J. O. Hirschfelder, Ch. F. Curtiss, B. B. Bird, *Molecular Theory of Gasses and Liquids* (Wiley, New York, Chapman and Hall, London, 1954), pp. 528, 534.
11. P. M. Holland, L. Biolsi, and J. C. Rainwater, *J. Chem. Phys.* **85**:4011 (1986).
12. V. I. Dolgov and V. S. Yargin, *Teplofiz. Vysokikh Temp.* **24**:1017 (1986).
13. A. O. Erkimbaev and A. M. Semenov, *Teplofiz. Vysokikh Temp.* **24**:1090 (1986).
14. V. S. Yargin, G. I. Belashova, and V. I. Dolgov, in *Thermophysical Properties of Working Fluids, Heat-Transfer Agents and Structural Materials in Modern Power Engineering* (Moscow Institute of Power Engineering, Moscow, 1985), pp. 62–68.
15. M. L. Olson and D. D. Konowalow, *Chem. Phys.* **21**:393 (1977).
16. D. D. Konowalow and M. L. Olson, *J. Chem. Phys.* **71**:450 (1979).
17. D. D. Konowalow, M. E. Rosenkrantz, and M. L. Olson, *J. Chem. Phys.* **72**:2612 (1980).
18. D. D. Konowalow and M. E. Rosenkranz, *J. Chem. Phys.* **86**:1099 (1982).
19. D. L. Timrot, V. V. Makhrov, and F. I. Pilnensky, *Teplofiz. Vysokikh Temp.* **22**:40 (1984).
20. D. D. Konowalow and M. E. Rosenkranz, *ACS Symp. Ser. (Metal Bonding and Interact. High-Temp. Syst.)* **179**:3 (1982).